Journal of Engineering Science and Technology
Vol. 12, No. 4 (2017) 898 - 912

EXPERIENTIAL INVESTIGATION OF TWO-WAY CONCRETE SLABS WITH OPENINGS REINFORCED WITH GLASS FIBER REINFORCED POLYMER BARS

MOHANAD T. ABDULJALEEL[1], AKRAM S. MAHMOUD[1,*], ALI R. YOUSIF[2]

[1]Civil Engineering Department, Engineering College,
Anbar University, Ramadi City, Anbar province, Iraq
[2]Civil Engineering Department, Engineering College, Salahaldin University, Erbil, Iraq
*Corresponding Author: dr.akramsh1@uoanbar.edu.iq

Abstract

This research had focused on glass fiber reinforced polymer (GFRP) reinforced concrete flat plate slabs with symmetrical openings. The results of ten interior slab-column connections were presented and discussed. The test parameters are reinforcement ratio, reinforcement type, and openings location. The specimens had been tested under monotonic concentric loading up to failure. The result showed that increasing the reinforcement ratio resulted in higher punching shear-shear capacity, lower deflection, and lower reinforcement ratio. Existing of openings reduced the punching shear capacity, and increased of the deflection, for instance, when spaced of opening's location form column face up to three times of effective depth, it will be issued to increase 25% of punching strength in slab.

Keywords: GFRP bars, Flat plate slab, Punching shear, Openings, Strain.

1. Introduction

Durability of reinforced concrete structure is a major concern in the construction of building. In aggressive environmental the corrosion of steel bars is a huge challenge for designer and engineering. Corrosion of steel increases the volume of bars and causes cracking and spalling of the concrete cover, which will short the life of building. An extensive study has been done, about the durability term and the corrosion of steel, for instance increasing the concrete cover, epoxy coating, stainless steel, none of these solution has been proven to be a good solution [1]. For instance, FRP has brittle liner elastic response, lower modulus of elasticity, different bond characteristic than that of steel reinforcement.

Nomenclatures

b_o	Perimeter critical section for slabs at distance 0.5*d* from column face, mm
D	Effective depth of slab, mm
d	Slab thickness, mm
E_f	Modulus of elasticity of FRP, MPa
E_s	Modulus of elasticity of Steel, MPa
$f_c^{'}$	Specified compressive strength of the concrete, MPa
l_1	Shortest span of two-way flat slab, m
l_2	Longest span of two-way flat slab, m
U	Perimeter of the loaded area, mm
v_u	Stress at (0.5*d*) from column face, MPa
X_{cone}	Distance from column face to observed failure, calculated by average around the column, mm

Greek Symbols

α_s	A factor equals to 4.0 for interior column, 3.0 for edge column, and 2.0 for corner column
β_c	Ratio of long side to short side of the column
γ_b	Safety factor
Δ_u	Deflection at mid-span, mm
ε	Strain at ultimate load, mm/mm
λ	Factor to account for low-density concrete (1.0 for normal weight concrete)
ρ_f	FRP reinforcement ratio
ϕ_c	Resistance factor for concrete (0.65)

Abbreviations

ACI	American Concrete Institute
CSA	Canadian Standards Association
FRP	Fibre Reinforced Polymer
GFRP	Glass Fibre Reinforced Polymer
JSCE	Japan Society of Civil Engineers

FRPs still new reinforcement materials, but also have more than one application; one of these applications is flat slab building. The failure in this system commonly occurs at the slab column connection.

In flat plate system, normally slab is directly supported by a column which will allow the forces and loads to be transferred from slab to column. This condition might create a critical zone around column. In flat plate slab the failure is brittle and with limited deflection. This type of failure called punching shear. FRP appeared in the market in the early 1990's as another solution to corrosion problem. Several ways were used to increase the punching shear capacity of slab-connection such as increasing slab thickness, concrete strength, column dimension, using drop panels, column heads, and shear reinforcement. GFRPs bars are alternative reinforcement to conventional steel bars for concrete structure under hard environmental conditions. The application of GFRP bars in RC two-way slabs is very limited especially with openings at column connection. In

addition, there is a lack of research and data on the punching shear of slabs reinforced with GFRP and with openings. Therefore, experimental results on flat plat slabs with opening are needed to understand the behaviour of structure of such element.

Flat plate slabs have more than one advantage but also some time can be dangerous because of the brittle and sudden failure. Locating openings at vicinity of slab column connection may lead to collapse of the floor if the requirement of design is not satisfied. For purposes of design, slab systems are divided into column and middle stirrups in each direction. The column strip width at each side of the column is equal to 1/4 of the length of shorter span. The middle strip is bounded by two column strips. ACI code gives the limitations of openings which include the size and the location. These guidelines are illustrated in Fig. 1 for slab $l_2 \geq l_1$ [2].

Existing of the opening within 10 times the slab thickness from concentrated load or reaction support affects the shear capacity and flexural requirement.

Steel reinforcement interrupts the opening must be replaced on each side of the opening [2]. The effect of opening is evaluated by reducing the perimeter of the critical section (b_o) by length equal to the projection of the opening enclosed by two lines extending from the centroid of the column and tangent of the opening. ACI code gives the limitation of opening for flat plate slabs as following [3]:

- In the area common to the intersections of middle strips, openings of any size area permitted.
- In the area common to the intersection of column strips, the maximum permitted opening size is 1/8 the width of column strip in either span.
- At the intersection of one column strip and one middle strip, not more than 1/4 of the reinforcement in either strip shall be interrupted by opening.
- If an opening is located within a column strip or closer than 10h from concentrated load or reaction area, apportion of (b_o) enclosed by straight lines shall be considered ineffective.

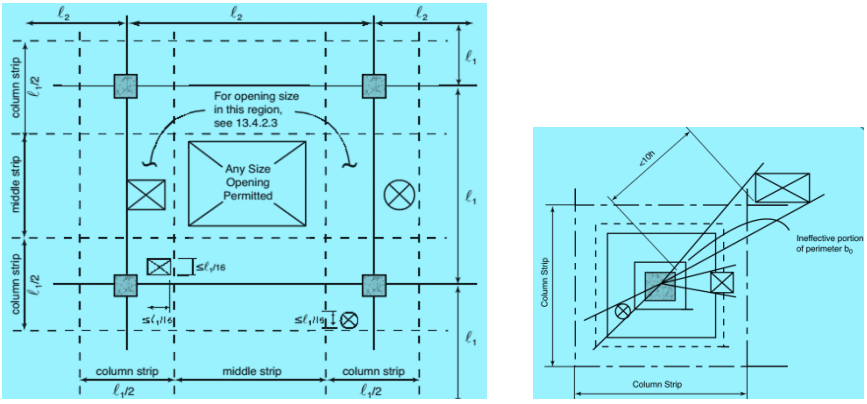

(a) Opening location and size. **(b) Reduction to perimeter of critical section b_o.**

Fig. 1. Flat slab with openings in column strips [2].

2. Literature Review

Punching shear failure is a local phenomenon, which generally occurs in a brittle behavior at the concentrated load or column connection region. This type of failure does not appear any external signs before the failure and occurs suddenly. A typical flat slab punching shear failure is characterized by punching of a column through a portion of the surrounding slab. This type of failure is more critical when determining the thickness of flat slab at a column connection. Therefore, the design of flat slab shall be safe and the accurate prediction of shear strength is a major concern [4].

Slab-column connections reinforced with FRP bars are a new application for hard environmental condition. FRP reinforced concrete have been covered by many codes and guidelines, Japan, Canada, USA, Euro code, and proposed equations [5-9]. The development has been done by modification of the existing steel reinforced concrete code.

2.1. American design guidelines

The American concrete institute (ACI) design guidelines for structural concrete reinforced with FRP bars are based on modifications of the ACI 318 steel reinforcement's code. The basis for this document is the knowledge gained from worldwide experimental research, analytical research work, and field applications of FRP reinforcement. The recommendations in this document are intended to be conservative. The subcommittee ACI 440.1R proposed equation for the shear transfer in two-way concrete slabs [5]. This equation considers the effect of the reinforcement stiffness as follow:

$$V_{c_{(ACI\,440)}} = 0.8\sqrt{f_c^{`}}\;\; b_o\, d\, k \tag{1a}$$

$$k = \sqrt{2\rho_f\, n_f + \left(\rho_f\, n_f\right)^2} - \rho_f\, n_f \tag{1b}$$

$$n_f = E_f / E_c \tag{1c}$$

where b_o is the perimeter of critical section for slabs at distance 0.5d from column face (mm), d is slab thickness (mm), ρ_f is the FRP reinforcement ratio, and E_f and E_s are the modulus of elasticity of FRP and steel, respectively, and $f_c^{`}$ is the specified compressive strength of the concrete (MPa).

2.2. Canadian code design

Design method in the Canadian Standards Association (CSA) code is based on limiting a shear force that can be resisted along a defined failure surface, with the concrete contribution taken as proportional to the square root of the concrete compressive strength [6]. The CSA code calculates the critical section at a distance of d/2 from the concentrated load. Canadian standard association gave equations for predicting the punching shear strength of FRP-RC as shown below [7]:

$$V_{c_{(CAN/\,CSA)_{S806-12}}} = 0.028\lambda\, \emptyset_c \left(1 + \frac{2}{\beta_c}\right) \left(E_f\;\; \rho_f\, f_c\right)^{1/3} b_{o;0.5d}\, d \tag{2}$$

$$V_{c_{\left(\frac{CAN}{CSA}\right)_{S806-12}}} = 0.147\lambda\, \emptyset_c \left(\frac{\propto_s d}{b_{o:0.5d}} + 0.19\right) \left(E_f\ \rho_f\, f_c\right)^{\frac{1}{3}} b_{o;0.5d}\, d \tag{3}$$

$$V_{c_{(CAN/\,CSA)_{S806-12}}} = 0.056\lambda\, \emptyset_c\ \left(E_f\ \rho_f\, f_c\right)^{1/3} b_{o;0.5d}\, d \tag{4}$$

where λ is a factor to account for low-density concrete (1.0 for normal weight concrete), ϕ_c is the resistance factor for concrete (0.65), β_c is the ratio of long side to short side of the column, and α_s is a factor equals to 4.0 for interior column, 3.0 for edge column.

2.3. Japanese code design

Japan society of civil engineers (JSCE) design guidelines are based on modifications of the Japanese steel RC code, and can be applied for the design of concrete reinforced or prestressed with FRP bars [8].

$$V_c = \beta_d\, \beta_p\, \beta_r\, f_{pcd}\, b_{o;0.5d}\, {}^{d}/_{\gamma_b} \tag{5a}$$

$$\beta_d = (1000/d)^{1/4}\ \leq\ 1.5 \tag{5b}$$

$$\beta_p = \left(100\rho_f E_f/E_s\right)^{1/3} \leq 1.5 \tag{5c}$$

$$\beta_r = 1 + 1/(1 + 0.25\, u/d) \tag{5d}$$

$$f_{pcd} = 0.2\sqrt{f_c^{`}} \leq 1.2\ \text{MPa} \tag{5e}$$

where u is perimeter of the loaded area (mm), and γ_b is safety factor.

2.4. Proposed equations by researchers

Due to the differences between FRP and steel reinforcement in terms of modulus of elasticity and bond characteristics, the application of steel reinforced concrete equations on FRP-reinforced concrete slabs is questionable, and it cannot be used directly to predict the punching capacity of slabs reinforced with FRP reinforcing bars or grids [9].

Researchers proposed a number of equations depended on the experimental results. El-Gamal et al. [1, 10] suggested the following equation:

$$V_{c_{(El-Gamal)}} = 0.33\sqrt{f_c}\ \ b_o\, d\ \propto\ (1.2)^N \tag{6a}$$

$$\propto = 0.5\left(E_f\ \rho_f\right)^{1/3} \left(1 + 8d/b_{o;0.5d}\right) \tag{6b}$$

where N is the continuity factor taken as zero for one panel slabs, 1 (for slab continuous along one axis), and 2 (for slabs continuous along their two axes).

Mathis and Tierce [11] suggested a modified equation of the British Standard as illustrated in Eq. (7):

$$V_{c_{(Matthys\ and\ Taerwe)}} = 1.36\ \frac{\left(100\rho_f \frac{E_f}{E_S} f_c\right)^{0.33}}{d^{0.25}}\ \ b_{o;1.5d}\, d \tag{7}$$

where ρ_f is the FRP reinforcement ratio, and E_f and E_s are the modulus of elasticity of FRP and steel, respectively.

3. Experimental Work

All specimens were casted in ambient conditions and demoulded at 24 ± 2 hours after casting and then cured at temperature 25 ± 2 °C until the age of testing.

3.1. Mechanical characterization of FRP bars

A (12.7 mm diameter) (No.13) deformed surface GFRP bars were used in this study. The tensile strength and modulus of elasticity of the GFRP bars were determined by testing. Figure 2 shows the typical stress-strain curve.

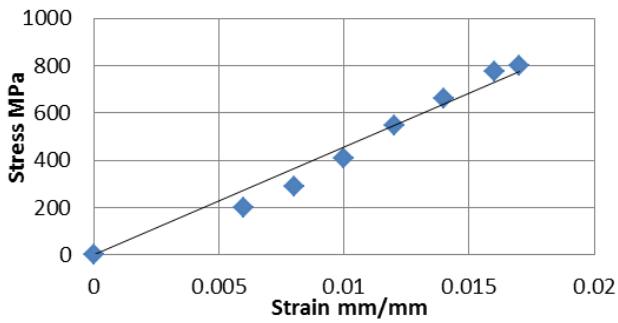

Fig. 2. Strain-stress relationships of GFRP bar.

3.2. Test specimens

Experimental work consisted of seven flat plate slabs which were designed to simulate the medium-scale of interior slab-column connection. It was found that the dimensions of (1100×1100×90) mm is proper to simulate slab-column connection, with GFRP diameter equal to 12.7 mm. The thickness of slab was kept constant with 90 mm for all specimens, concrete cover was 15 mm. The average effective depth (*d*) was 62mm. The test specimens were cast with normal-strength concrete, the concrete strength determined on the day of testing (determined on 150×300 mm cylinders) ranged from 28.9 to 37.3 MPa. Reinforcement ratio ranged from 0.5% to 2.2% for both types of bars. Figure 3 shows the dimensions and support details of the specimens. Table 1 shows the details of specimens. Figures (4 and 5) show the fabrication of the specimens.

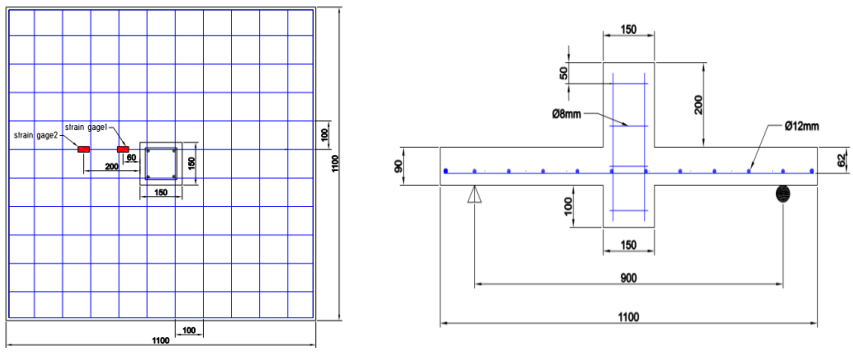

Fig. 3. Slab-column connection details.

Table 1. Details of flat plate slabs.

Speci-men	Reinf. of Steel bar	Reinf. of FRP bar	ρ	$\rho\left(\frac{E_f}{E_s}\right)$	f'_c MPa	Slab's opening location
SG1	-	12 Ø12	0.022	0.005	29.8	N/A
SS1	10 Ø12	-	0.016	0.016	35.8	N/A
SS2	7 Ø 8	-	0.005	0.005	28.9	N/A
SGO1	-	7 Ø12	0.013	0.003	37.3	At column face
SGO2	-	7 Ø12	0.013	0.003	32.6	2d from column face
SGO3	-	12 Ø12	0.022	0.005	30.5	At column face
SGO4	-	12 Ø12	0.022	0.005	35.4	2d from column face
SGO5	-	12 Ø12	0.022	0.005	30.1	3.5d from column face
SSO1	7 Ø 8	-	0.005	0.005	35.7	At column face
SSO2	7 Ø 8	-	0.005	0.005	30.5	2d from column face

Fig. 4. Specimens without openings

Fig. 5. Specimens with openings.

3.3. Test procedure

The deflection of test specimens at the mid-span was measured by dial gauge, while the strains in flexural reinforcement bars located at critical zone. The strain gauges connected to a data-logger to record the readings during the test. Crack

propagation was marked during the test and the corresponding loads were recorded. Figure 6 shows the specimen installation. The test specimens were simply supported achieved by frame with circular bar to create line supports. Circular bar was covered by thick rubber along four edges to give uniform load and to prevent local failure. The load was applied from the top of slab through 150×150 mm column stub by using digital machine for multiuse with capacity 600 kN at a loading rate of 5 kN/min until failure. A total of six slabs had deformed-surface GFRP bars as flexural reinforcement, while 4 specimens had traditional steel bars as reference specimens.

4. Test Results

Ten slab-column connections were tested under monotonic concentric loading until failure. The laboratory test results are limited to punching-shear capacity and strain in reinforcing bars since main objective of this study us to understand the behaviour of two-way concrete slabs reinforced with GFRP bars. The results presented herein are limited to the punching-shear capacity and the strains in the reinforcing bars. Different specimens show different behaviour during test according to their strength and stiffness. Summaries of test data and results are presented in Table 2.

Fig. 6. Specimen installation.

Table 2. Summary of the test results.

Specimen	ρ %	$\rho\left(\frac{E_f}{E_S}\right)$	V_u kN	Δ_u mm	$\frac{v_u}{\sqrt{f\grave{c}}}$	$\frac{V_u}{\sqrt{f\grave{c}}}$	X cone	Strain at Ultimate Load $\mu\varepsilon$
SG1	2.2	0.51	136.2	16.20	0.47	24.9	3.6*d*	7120
SS1	1.6	1.6	178	10.70	0.56	29.7	4.2*d*	3064
SS2	0.51	0.51	100	12.50	0.35	18.6	2.7*d*	-
SGO1	1.3	0.3	67.7	14	0.42	11.0	2.4*d*	7935
SGO2	1.3	0.3	85	20.80	0.34	14.8	2.9*d*	-
SGO3	2.2	0.51	80	17.70	0.55	14.4	4.0*d*	7757
SGO4	2.2	0.51	100	11.30	0.39	16.8	3.4*d*	4691
SGO5	2.2	0.51	102	13.55	0.40	18.5	2.4*d*	-
SSO1	0.51	0.51	77.1	12.30	0.49	12.9	2.2*d*	-
SSO2	0.51	0.51	85	12.45	0.36	15.3	3.0*d*	-

4.1. Punching shear capacity

All slabs failed by punching shear at different load capacity. The punching shear capacity and punching shear stress at failure were normalized to the square root of concrete strength to account for variation in the concrete strength. The large difference between the ultimate strength of SS1 and SGO1 attributes to the reinforcement ratio, openings, and modulus of elasticity.

The most effective one is the modulus of elasticity where the modulus of elasticity of Steel and GFRP bars are 200 GPa, 45 GPa respectively, the value of (E_f/E_s) equal to0.25. Existence of opening caused a reduction in the ultimate capacity of slab due to decrease in (b_o) parameter which is important for punching phenomenon.

The reinforcement type affects the punching shear capacity of specimens see SS1 and SG1 specimens. Beside the difference in modulus of elasticity between the GFRP and steel bars, the bond properties are also different. Using GFRP reinforcement ratio equal to steel reinforcement ratio yielded smaller neutral axis depth as well as higher strain and wider cracks at same load value [6]. Thus, contribution of un-cracked zone up the neutral axis and aggregate interlock decreased, which yielded lower punching shear capacity.

4.2. Reinforcement ratio effect

Depending on the experimental test results, increasing the reinforcement ratio increased the punching shear capacity. Figure 7 shows the effective reinforcement ratio versus the normalized stress.

For slabs without openings, increasing reinforcement ratio of steel bars from 0.51% to 1.6% increased the normalized stress by 37.3%. For slabs with openings, reinforcement was added around the openings by approximately two times the reinforcement which had been cut. The reinforcement was added around the openings mainly to overcome cracks at opening corners and to reduce the reduction in punching capacity. For specimens SGO2 and SGO4 which were reinforced with GFRP bars and with openings, increasing reinforcement ratio from 1.3% to 2.2% increased the normalized stress by 12.9%. For specimens SGO1 and SGO3 which were reinforced with GFRP bars and with openings, increasing reinforcement ratio from 1.3% to 2.2% increased the normalized stress by 23.6%.

4.3. Load-deflection response

Load- deflection relationships are important to understand the behaviour of slab-column connections because it reflects the general behaviour and especially the reinforcement ratio. Figure 8 shows the load-deflection relationships of specimens without openings. The curve shows clear difference between both specimens, specimen SS1 with 1.6% reinforcement showed more brittle behavior and sudden failure at ultimate load of 178 kN. While specimen SS2 with 0.5% reinforcement ratio showed some plastic behavior and then punching shear failure at ultimate load of 100 kN. All specimens showed a short linear elastic behavior, and after the first cracking the stiffness was strongly reduced as shown in curves of load-deflection.

For specimen SS2, clear changing of stiffness observed at load of about 50 kN due to the low reinforcement ratio. GFRP specimen SG1 showed sudden failure similar to SS1. The difference in slab stiffness is clear between GFRP and steel specimens, for instance at specific loading level, GFRP specimen showed higher deflection

Existing of the openings affected the load-deflection behavior and change the behavior of specimen toward more ductile manner. Increasing the reinforcement ratio increased the stiffness of the specimens and enhances the load carrying capacity. The increasing of the reinforcement ratio had decreased the deflection at specific loading level. Existing of openings at column face gave higher deflections at specific loading, for instance SGO1 showed lowest capacity and highest deflection because the cut-off reduced the ductility and stiffness of specimen. Figure 9 shows the load-deflection relationships of specimens with openings.

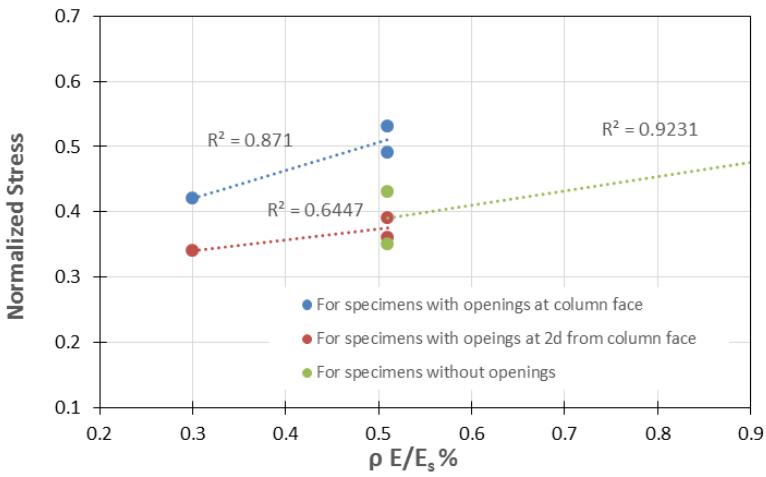

Fig. 7. Normalized punching shear stress versus the axial stiffness of reinforcements.

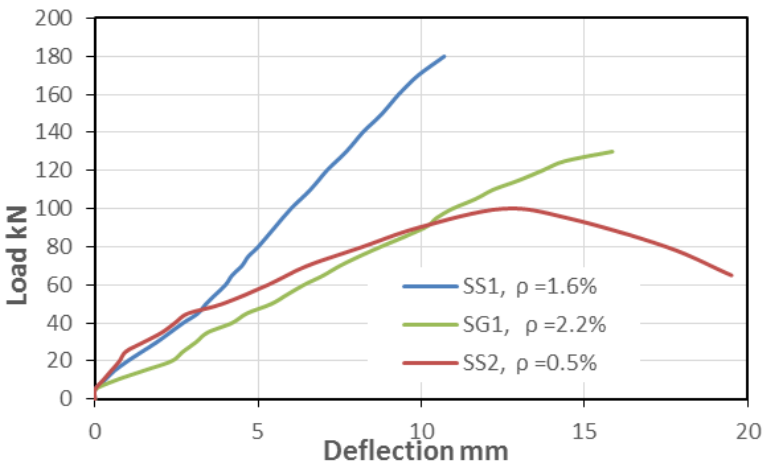

Fig. 8. Load-deflection relationships for specimens without openings.

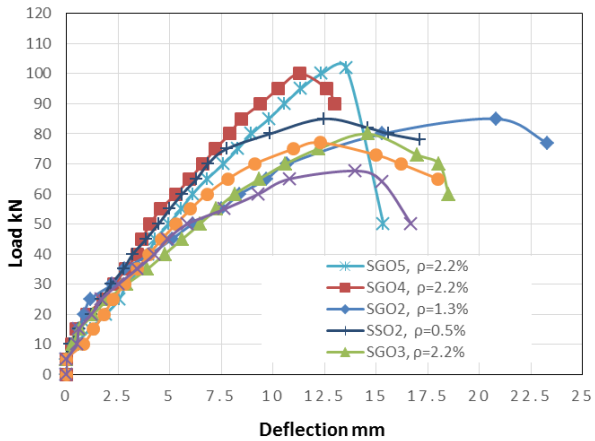

Fig. 9. Load-deflection relationships for specimens with openings.

4.4. Cracks pattern and failure mode

All specimens failed by punching shear, three specimens SS1, SG1, and SGO5 failed in brittle mode. At load levels between 15 and 35kN, the first crack appeared on tension side of slabs. The cracks started from column sides and extended toward the edges of slabs. At a high load level, the circumferential cracks appeared in the vicinity of the column. At the final stage of loading, the rate of formation of new cracks decreased significantly and existing cracks grew wider. For steel reinforcement specimens, increasing reinforcement ratio from 0.5% SS2 to 1.6% SS1 resulted in a wider failure surface, due to enhancement of the restraint in the plane of the slab as a result of increased flexural reinforcement. For GFRP specimens, increasing reinforcement ratio from 1.3% to 2.2% resulted in more cracks but with less spacing, this attributed mainly to the reduced the spacing of bars and distribution of stress on more bars. Researchers reported that the crack width and spacing are directly proportional to the spacing between slab reinforcement bars and to the concrete cover thickness [12]. Specimens with low reinforcement ratio 0.5% of steel and 1.3% of GFRP bars, showed more ductile failure with wider cracks. For specimens with openings, the cracks were concentrated at the sides of openings due to the high stress effect.

In general, specimens reinforced with GFRP bars had shown wider cracks. Wider cracks of compression side have been observed when the openings were close to the column face especially at distance (2*d*) which it measured from column face and with low reinforcement ratio. Figure 10 shows the failure mode of some specimens

4.5. Strain measurements

Strain of flexural GFRP reinforcement and steel bars were measured by electrical strain gauges. Two strain gauges were located on GFRP bars at critical location of each slab-column connection. The strain in GFRP bars was not similar to that of steel bars. Linear responses for all specimens were observed before the first crack, as shown in Fig. 11. After fist cracks, the change in load-strain behavior was observed and the strain was increased with load increasing. For GFRP specimens,

large strains were recorded predicted compared to the steel specimen; the maximum strain was (8000 $\mu\varepsilon$) for specimen SGO1. This attributes to material properties and specially the modulus of elasticity of GFRP. All strains were measured up to the ultimate load, except for specimens SS2, SSO1, SSO2, and SGO4 which showed unreliable reading due to the gauges damage.

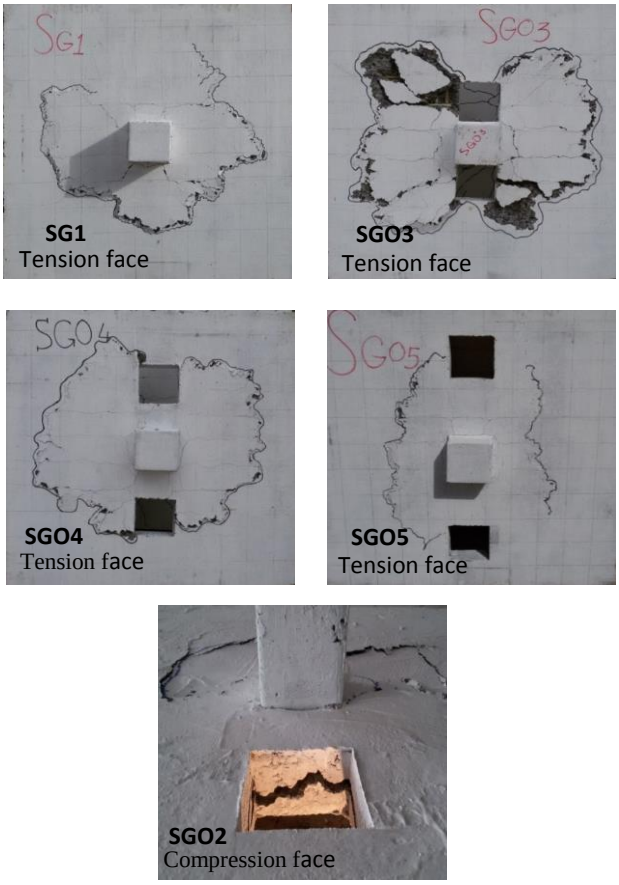

Fig. 10. Failure mode strain.

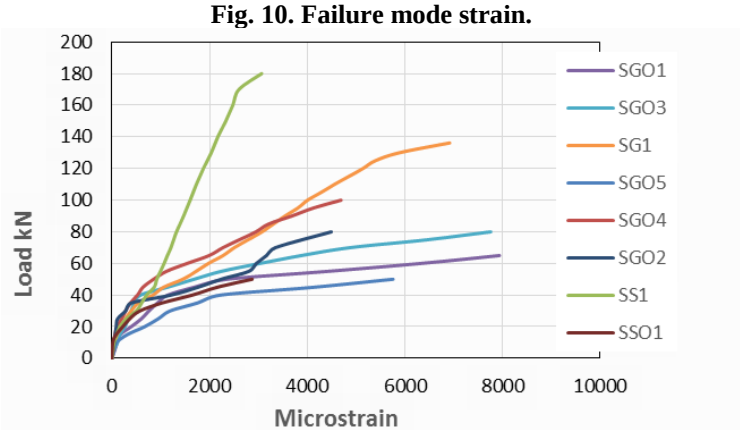

Fig. 11. Strain vs. load relation-ships of tested specimens.

5. Predications of Punching Shear Capacity of Slabs without and with Openings Reinforced with GFRP Bars

Experimental result showed differences between the specimens which reinforced with GFRP and those with steel bars. Two equations were provided by ACI 440 and Japan design recommendations, which have been intended for calculating the punching shear capacity [5-9]. In addition, the researchers in references [10-12] proposed equations based on their experimental investigations to predict the punching capacity of FRP RC members. Many equations were derived depending on the modification of the mechanical properties by factor $\left(E_f/E_s\right)^{1/3}$. All previous codes and prosed equations are proposed mainly for solid slabs. Canadian standard association recently proposed a new equation in the 2012 edition of CSA in section of 806. The accuracy of this equation has been test in this chapter. Table 3 summarizes the punching shear capacity prediction by the equations used for GFRP reinforced concrete slabs.

Comparison between experimental and predicted shear capacity

Table 3 presents the ratio between the experimentally measured and predicated capacity ($V_{exp.}/V_{pred.}$) using ACI 440 [5], CSA [7], JCEC [8], El-Gamal et al. [10] and Matthys and Taerwe [11] equations. The factor of safety was set to 1.0 for all equations. As shown in Table 3, all equations yielded good and conservative predictions with ACI 440 predictions being more conservative in comparison to the other guideline. The equation proposed by Matthys and Taerwe [11] showed more acceptable prediction with smallest mean of 1.3 and COV of 13%.

In general CSA S806-12, Matthys and Taerwe and El-Gamal et al. yielded good predictions of punching shear capacity.

Table 3. Experimental to predicate punching shear capacity ($V_{exp.}/V_{pred.}$).

Specimen	ACI 440 [5]	CAN/CSA S806-12 [7]	JSCE [8]	El-Ghandour et al. [10]	Matthys and Taerwe [11]
SG1	2.4	1.49	1.55	2.33	1.38
SGO1	2.83	1.63	1.5	2.07	1.48
SGO2	2.27	1.31	1.64	1.71	1.2
SGO3	2.8	1.74	1.61	2.7	1.6
SGO4	2.07	1.29	1.29	1.19	1.15
SGO5	2.06	1.26	1.3	1.22	1.16
Mean	2.40	1.45	1.58	1.7	1.31
S.D.	0.34	0.19	0.28	0.45	0.17
COV%	14	13	18	26	13

6. Conclusions

The main conclusions derived from this study may be summarized as follows:

- Regardless of the reinforcement type and ratio, the final mode of failure in all tested specimens was punching shear failure. The specimens with low

reinforcement ratio showed large plastic deformation before the punching shear failure.

- Increasing the reinforcement ration of the two types yielded higher punching shear capacity and lower strain in the reinforcement.
- No bond failure was seen for all slab-column connection specimens.
- Locating the openings at column face and at distance 2d from column face leads to crushing of concrete in the compression zone.
- The initial cracking load for steel reinforced specimen was higher than that of the GFRP reinforced specimen.
- Regardless of the reinforcement type, increasing the reinforcement ratio decreased the strain in the reinforcement bar.
- The maximum distance between the column face and failure surface (X cone) was 4.2d for specimen SS1, the minimum of (X cone) was 2.2d for specimens SSO1, while the ACI code permit only 0.5d from column face to the critical perimeter.
- CSA S806-12, Matthys and Taerwe [11] and El-Gamal et al. [10] proposed equations yielded good predictions of punching shear capacity when compared to the experimental results.
- ACI 440 equation yielded very conservative results when compared to the experimental results.

References

1. El-Gamal, S.E.; El-Salakawy, E.F.; and Benmokrane, B. (2005). A new punching shear equation for two-way concrete slabs reinforced with FRP bars. *International Concrete Abstracts Portal, Special Publication*, 230, 877-894.
2. Anonym (2006). *An engineer's guide to: openings in concrete floor slabs*. Portland Cement Association, Skokie, Illinois, USA, 1-4.
3. ACI 318-14; (2014). *Building code requirements for structural concrete*. American Concrete Institute, Farmington Hills, MI, USA.
4. Fico, R. (2007). *Limit states design of concrete structures reinforced with FRP bars*. Ph.D. Thesis. Department of Structural Engineering, Naples Federico University, Italy.
5. ACI 440.1R (2006). *Guide for design and construction of concrete reinforcement with FRP bar.* American Concrete Institute, Farmington Hills, MI, USA.
6. Hassan, M.; Ahmed E.A.; and Benmokrane, B. (2014). Punching-shear design equation for two-way concrete slabs reinforced with FRP bars and stirrups. *Construction and Building Materials*, 66, 522-532
7. CAN/CSA S806 (2012). *Design and construction of building structures with fiber reinforced polymers.* The Canadian Standards Association, Ontario, Canada, 150-198 .
8. Machida, A.; and Uomoto, T. (1997). *Recommendation for design and construction of concrete structures using continuous fibre reinforcing*

materials. Concrete Engineering Series 23, Japan Society of Civil Engineers, JSCE, Tokyo, Japan, 1-325.

9. Ospina, C.E.; Alexander, S.D.B.; and Cheng, J.J.R. (2003). Punching of two-way concrete slabs with fiber-reinforced polymer reinforcing bars or grids, *ACI Structural Journal*, 100(5), 589-598.
10. El-Gamal, S.; El-Salakawy, E.; and Benmokrane, B. (2005). Behaviour of concrete bridge deck slabs reinforced with fiber-reinforced polymer bars under concentrated loads. *ACI Structural Journal*, 102(5), 727-735.
11. Matthys, S.; and Taerwe, L. (2000). Concrete slabs reinforced with FRP grids. I: one-way bending. *Journal of Composites for Constructions*, 4(3), 145-153.
12. Sayed, A. (2015). *Punching shear behaviour of FRP-reinforced concrete interior slab-column connections*. Ph.D. Thesis. Department of Civil Engineering, University of Manitoba, Winnipeg, Manitoba, Canada.